T_g–Temperature Property (T_gTP) Diagram for Thermosetting Systems: Anomalous Behavior of Physical Properties vs. Extent of Cure

XIAORONG WANG and JOHN K. GILLHAM*

Polymer Materials Program, Department of Chemical Engineering, Princeton University, Princeton, New Jersey 08544-5263

SYNOPSIS

The relationships between the isothermal physical properties in the glassy state of amorphous thermosetting crosslinked polymers and chemical conversion are anomalous and complex. In this manuscript, a generalized framework for correlating the basic physical properties of a high-T_g thermosetting amine/epoxy system vs. extent of cure at isothermal temperatures from above T_g to deep in the glassy state is reported in terms of the T_g–Temperature Property (T_gTP) Diagram. The framework arises from consideration of the isothermal shear modulus and the isothermal physical aging rate vs. extent of cure, both of which display maxima and minima throughout a wide range of temperatures below T_g. Use of T_g as a direct measure of conversion results in linearization of the relationships between the temperatures of the maxima and minima of the physical properties and extent of cure in the T_gTP Diagram. The anomalous behavior is related to specific phenomena, such as the glass transition (vitrification) and the glassy-state β-transition (T_β), the temperatures of which change with conversion, and also to gelation. The different types of behavior of a property of the material vs. extent of cure correspond to different regions in the diagram. Such simple diagrams are intellectually useful for understanding the properties of materials for both undercured materials (with change of conversion) and fully cured materials (with change of stoichiometric ratio). © 1993 John Wiley & Sons, Inc.

INTRODUCTION

An understanding of the relationships between bulk properties and conversion is important for the ongoing development of thermosetting polymeric systems. The sensitivity and the one-to-one relationship between the conversion and the glass transition temperature (T_g) for thermosetting systems implies that T_g is an appropriate parameter for measuring the conversion during cure, regardless of the cure path.[1-4] Theoretical analyses of this relationship have been reported.[1,5]

The basic isothermal physical properties of epoxy glasses, such as the density, modulus, water absorption, and creep, change with increase of the extent of cure (as measured by time of cure, conversion, crosslinking density, or glass transition temperature).[6-19] Many experimental reports show[6,8-11] that the higher the extent of cure, the lower the density, the lower the modulus and the more water absorbed for different epoxy systems at 25°C. However, the opposite has also been reported for the density, which was found to increase with increase of T_g.[12] Other reports show that the relationship between density or modulus and conversion displays a maximum at room temperature for epoxy systems[13,19] as well as for cyanate ester/polycyanurate systems.[17,18] The location of the maximum was suggested to be related to gelation.[18,19] The manner in which the physical properties in the glassy state of thermosetting resins change with extent of cure is therefore controversial.

The basic physical properties of a material are interrelated.[13,17-22] The anomalous changes in the

* To whom correspondence should be addressed.

Journal of Applied Polymer Science, Vol. 47, 425–446 (1993)
 CCC 0021-8995/93/030425-22

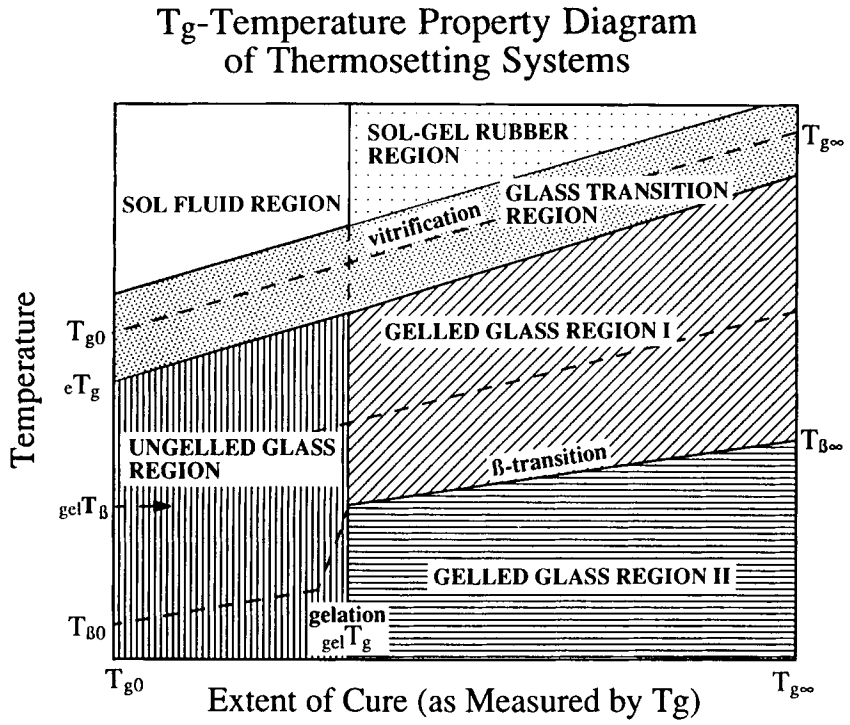

Figure 1 Schematic T_g–Temperature Property (T_gTP) Diagram for thermosetting systems. The physical properties of the curing system are determined by the different regions, which are separated by gelation ($_{gel}T_g$), and the transition contours for vitrification [the glass transition (T_g)], the end of the glass transition ($_eT_g$) and the β-transition (T_β) vs. extent of cure (see also Fig. 20). Anomalies occur isothermally when increasing conversion causes the material to pass from one region of the diagram to another.

density of a material vs. extent of cure implies that the modulus, water absorption, and creep, will also change anomalously with increasing extent of cure.

In practice, measurements of the density and water absorption for undercured systems are difficult to obtain throughout a wide temperature range because

CHEMICAL REACTANTS

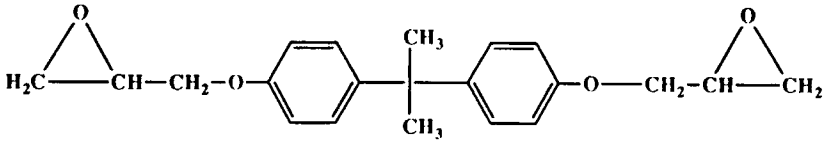

Diglycidyl Ether of Bis-phenol A

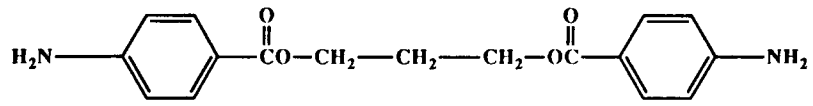

Trimethylene Glycol Di-p-aminobenzoate

Figure 2 Chemical structures of diglycidyl ether of bis-phenol A (DGEBA) and trimethylene glycol di-*p*-aminobenzoate (TMAB).

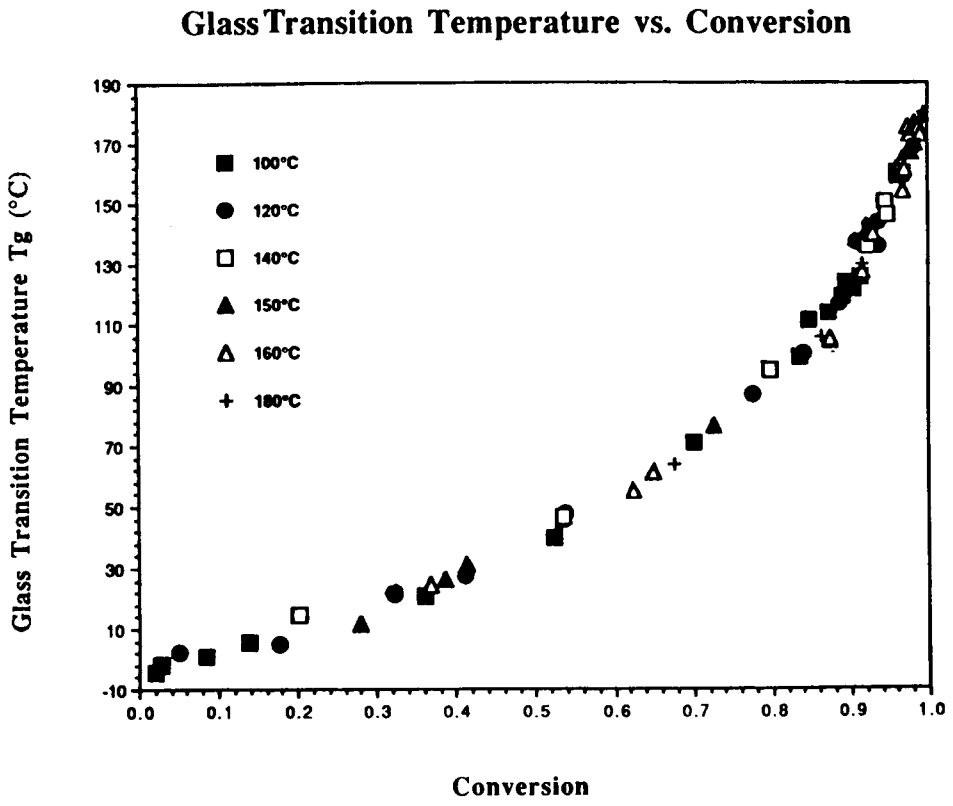

Figure 3 Glass transition temperature vs. chemical fractional conversion for a stoichiometrically equivalent DGEBA/TMAB system.[1,2]

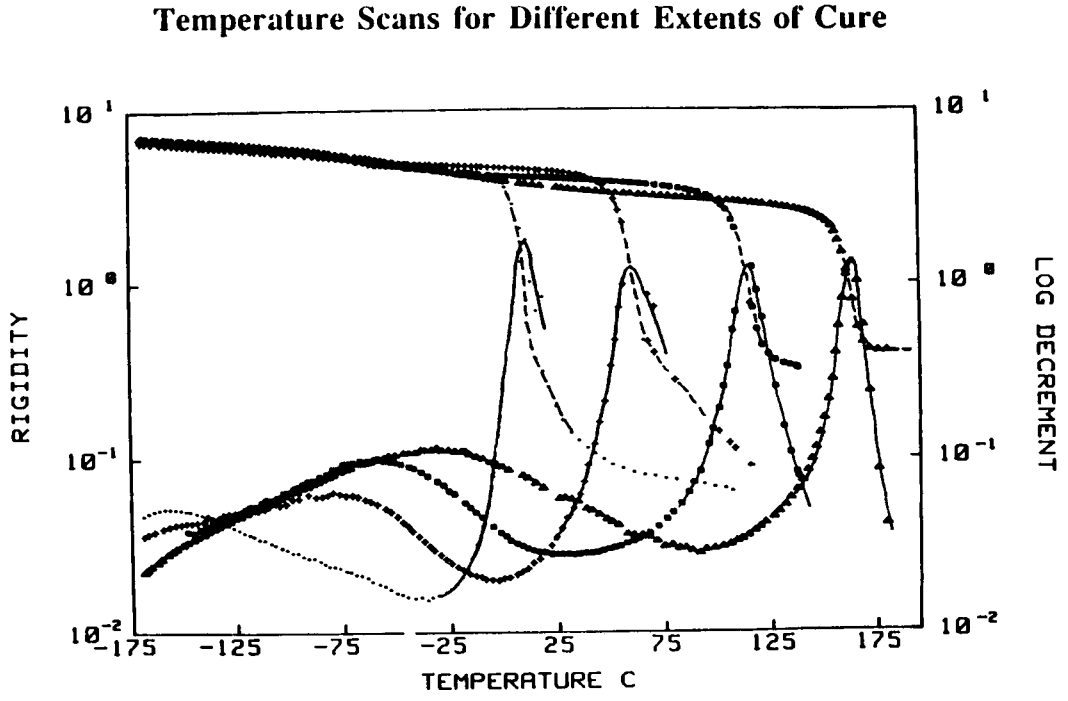

Figure 4 Dynamic thermomechanical behavior for the curing system for different extents of cure. Data were obtained on cooling after heating the specimen to successively higher temperatures (i.e., $T > T_g + 30°C$). T_g and T_β of the curing system are determined from the maxima in the logarithmic decrement (see Ref 23).

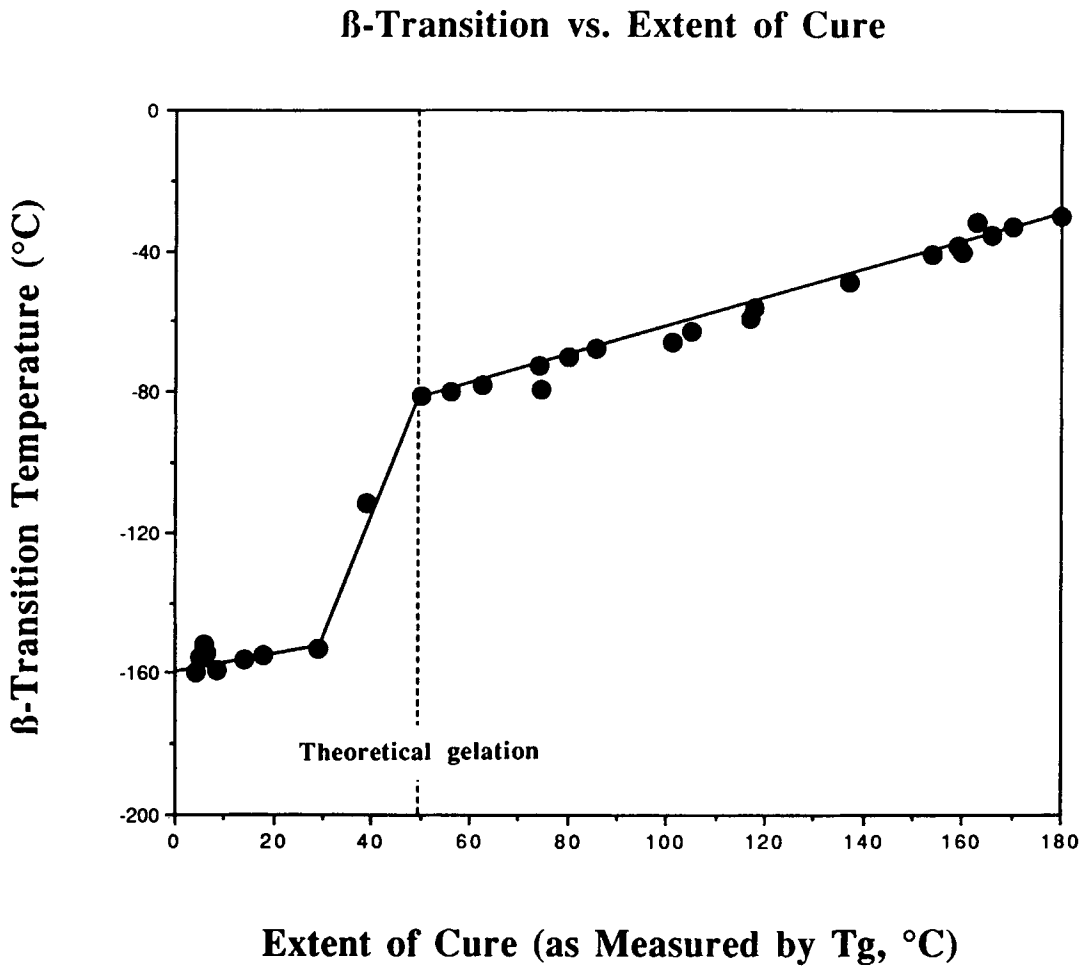

Figure 5 T_β vs. extent of cure (as measured by T_g).

of the extreme rheological changes that occur during transformation of liquid multifunctional monomer to solid crosslinked polymer. In contrast, relative modulus, obtained using the torsional braid analysis (TBA) technique,[6,23] is an appropriate parameter for measuring changes in the physical properties of thermosetting systems vs. extent of cure throughout a wide range of temperature (300°C in this work) and rheological behavior (liquid to glass in this work). In principle, a single TBA specimen can be used to obtain all of the thermomechanical data (relative modulus and mechanical loss), transition temperatures (T_g and T_β), and extents of cure (as measured by T_g), which thereby facilitates comparison of data.

In this article the study of a difunctional aromatic epoxy cured with a tetrafunctional aromatic diamine shows that the relationships of two basic physical properties vs. extent of cure at isothermal temperatures deep in the glassy state are complex functions with maxima and minima. Modulus and the rate of physical aging were the selected properties. Data were obtained using the TBA technique. A general framework for understanding and summarizing the relationships between properties and extent of cure at various temperatures from the liquid state to the glassy state is the T_g–Temperature Property (T_gTP) Diagram (Fig. 1; see also the discussion associated with Fig. 20). The X-axis of the diagram is labeled "extent of cure (as measured by T_g)" of the system. The Y-axis is labeled "temperature" of the system. The properties of the curing system may be separated into different regions (see Fig. 1) by the glass transition (T_g), the end of the glass transition ($_eT_g$) and the β-transition (T_β) vs. extent of cure and also by gelation ($_{gel}T_g$). The behavior of the physical properties of a material with respect to increasing cure is determined by its temperature and its T_g. Experimental data for the present system show that an increase of conversion (T_g) is equivalent to a decrease of temperature (and vice versa) with respect to change in physical properties. This conversion–temperature superposition implies that either conversion (T_g) or temperature can be used as the

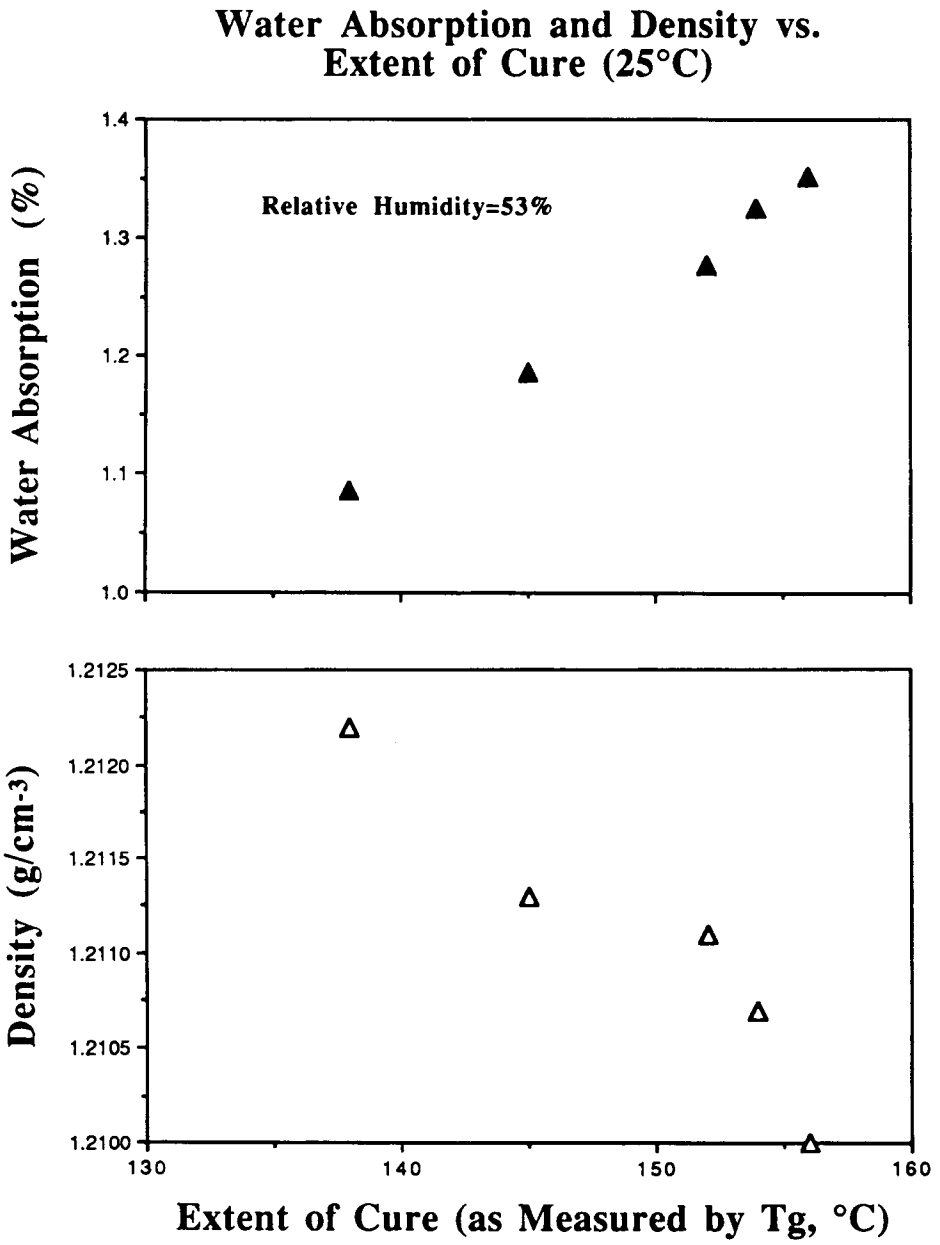

Figure 6 Water absorption and density vs. extent of cure (25°C).[8] The density is inversely related to water absorption.

independent variable. The diagram is developed using a high-T_g epoxy system, which has been previously investigated in this laboratory.[1,2] It is considered that the form of diagram applies to all thermosetting systems.

MATERIALS AND EXPERIMENTAL

Chemicals

The chemical system used was a liquid difunctional epoxy (diglycidyl ether of bisphenol A, DER 332, Dow Chemical Corp., "DGEBA") with a tetrafunctional aromatic diamine (trimethylene glycol di-*p*-aminobenzoate, "TMAB", Polaroid Corp.) (Fig. 2). The epoxy monomer is a viscous liquid at 25°C with an epoxide equivalent weight (EEW) of 174 g/eq. The amine curing agent is a highly crystalline solid (melting point = 125°C) with an amine hydrogen equivalent weight of 78.5 g/eq. The chemicals were stoichiometrically mixed at 100°C with vigorous stirring for 15 min in order to dissolve the amine in the epoxy resin. Immediately after mixing, the warm liquid was degassed for 10 min in a vacuum oven

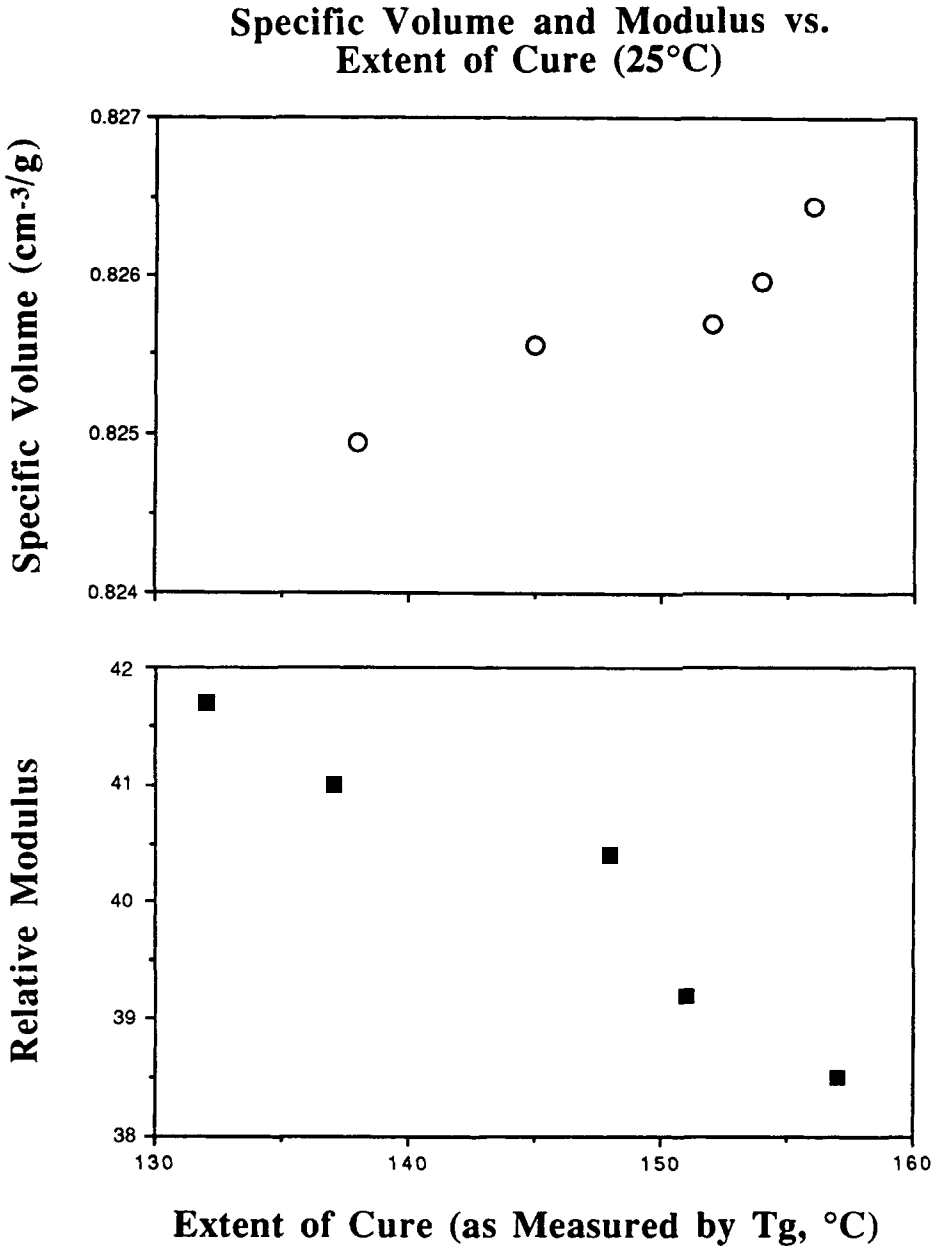

Figure 7 Specific volume and relative modulus vs. extent of cure (25°C).[8] The modulus is inversely related to specific volume (i.e., the modulus is proportional to density).

held at room temperature. The resulting clear viscous liquid mixture was stored at −15°C. The glass transition temperature of the initial mixture, T_{g0} = 0°C; the glass transition temperature of the fully cured material, $T_{g\infty}$ = 180°C; the β-transition temperature of the intial mixture, $T_{\beta 0} \simeq -160$°C; the β-transition temperature of the fully cured material, $T_{\beta\infty}$ = −35°C; the glass transition temperature of the material at its theoretical gelation point,[1,2] ${}_{gel}T_g \simeq 50$°C [evaluated from Flory's theory of gelation and the T_g/conversion relationship[1,2]]; the β-transition temperature of the material at its theoretical gelation point, ${}_{gel}T_\beta \simeq -75$°C (see below).

Specimen Preparation

A heat-cleaned glass braid was dipped in the viscous reactive liquid mixture at room temperature for 30 min; the impregnated glass braid was squeezed between aluminum foil to remove excess material and to insure good wetting of the glass filaments. The final amount of material on the braid was approximately 15 mg. The specimen was mounted to form

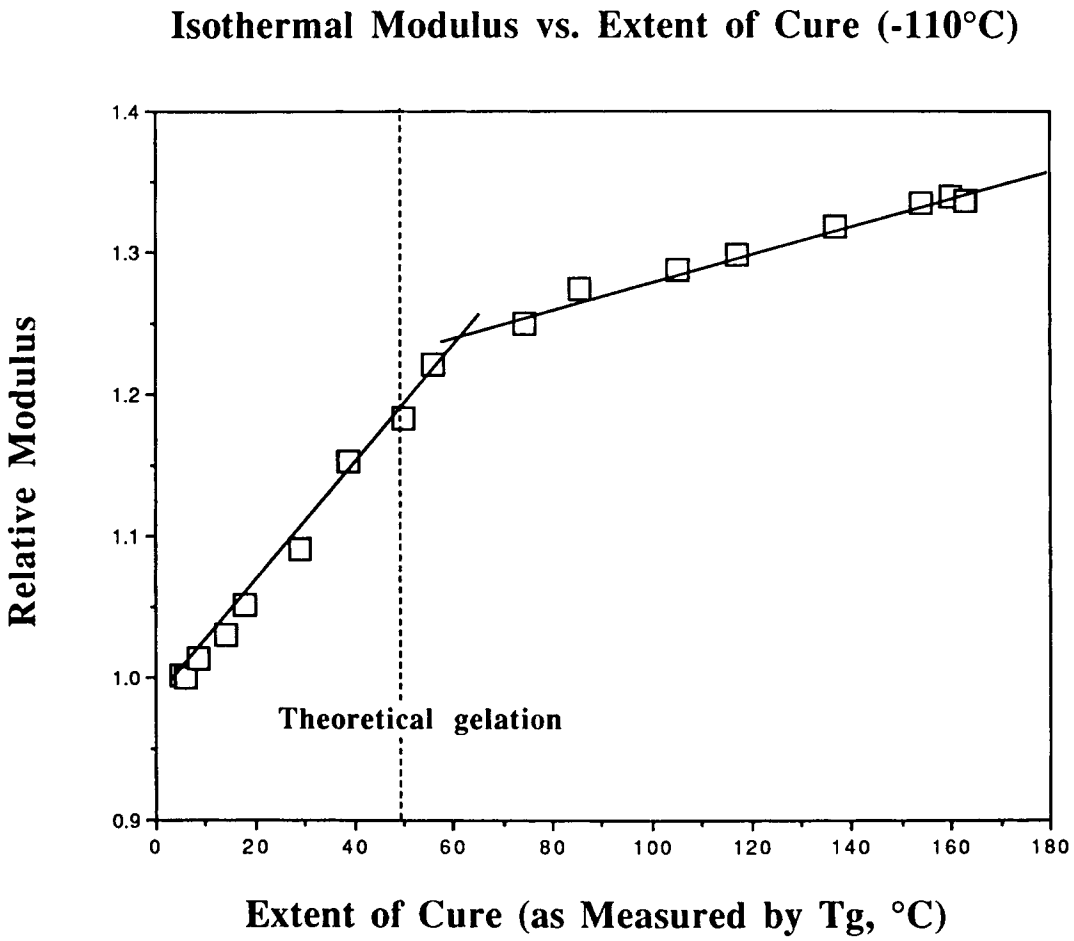

Figure 8 Isothermal relative modulus (−110°C) vs. extent of cure. The theoretical gelation value for T_g is evaluated from Flory's theory[26,27] and the T_g/conversion[1,2] experimental relationship.

the TBA inner pendulum, which was inserted into the preheated chamber of the TBA instrument (40°C). All subsequent experiments were performed in an atmosphere of flowing helium. Reviews of the TBA technique have been published.[6,23] The frequency of the freely damped oscillations was about 1 Hz. The sensitivity of the technique ($T < T_g$) is 0.01% of the property being measured (i.e., relative rigidity and mechanical damping expressed as logarithmic decrement). The automated TBA torsion pendulum system is available from Plastics Analysis Instruments, Inc., Princeton, NJ.

Modulus vs. Extent of Cure

An uncured specimen was initially heated to 140°C at 5°C/min and was then cooled at 1.5°C/min through the glass transition to −180°C. Dynamic mechanical measurements were obtained during the cooling (designated as the *preaged process*, in which physical aging effects are minimized; the T_g obtained during cooling is designated as the *preaged* T_g), which provided the relative rigidity and mechanical damping vs. temperature and assignments for T_g and T_β. The specimen was then heated to above its T_g to permit further cure. One specimen was used for obtaining all of the relative modulus vs. extent of cure (i.e., T_g) data at different temperatures by repeating the procedure many times. For isothermal modulus vs. extent of cure experiments, the relative modulus = G'_c/G'_u, where G'_u = rigidity of the uncured specimen, and G'_c = rigidity of the cured specimen. For isothermal physical aging experiments, the relative modulus is defined relative to the modulus of the unaged specimen at the aging temperature.

Physical Aging vs. Extent of Cure

A specimen was initially heated to a temperature about 100°C above the initial glass transition temperature (T_{g0}), and was then quenched, at 5°C/min, through the glass transition to the isothermal aging temperature ($T < T_g$, e.g., $T = T_g - 30$, $T_g - 50$, T_g

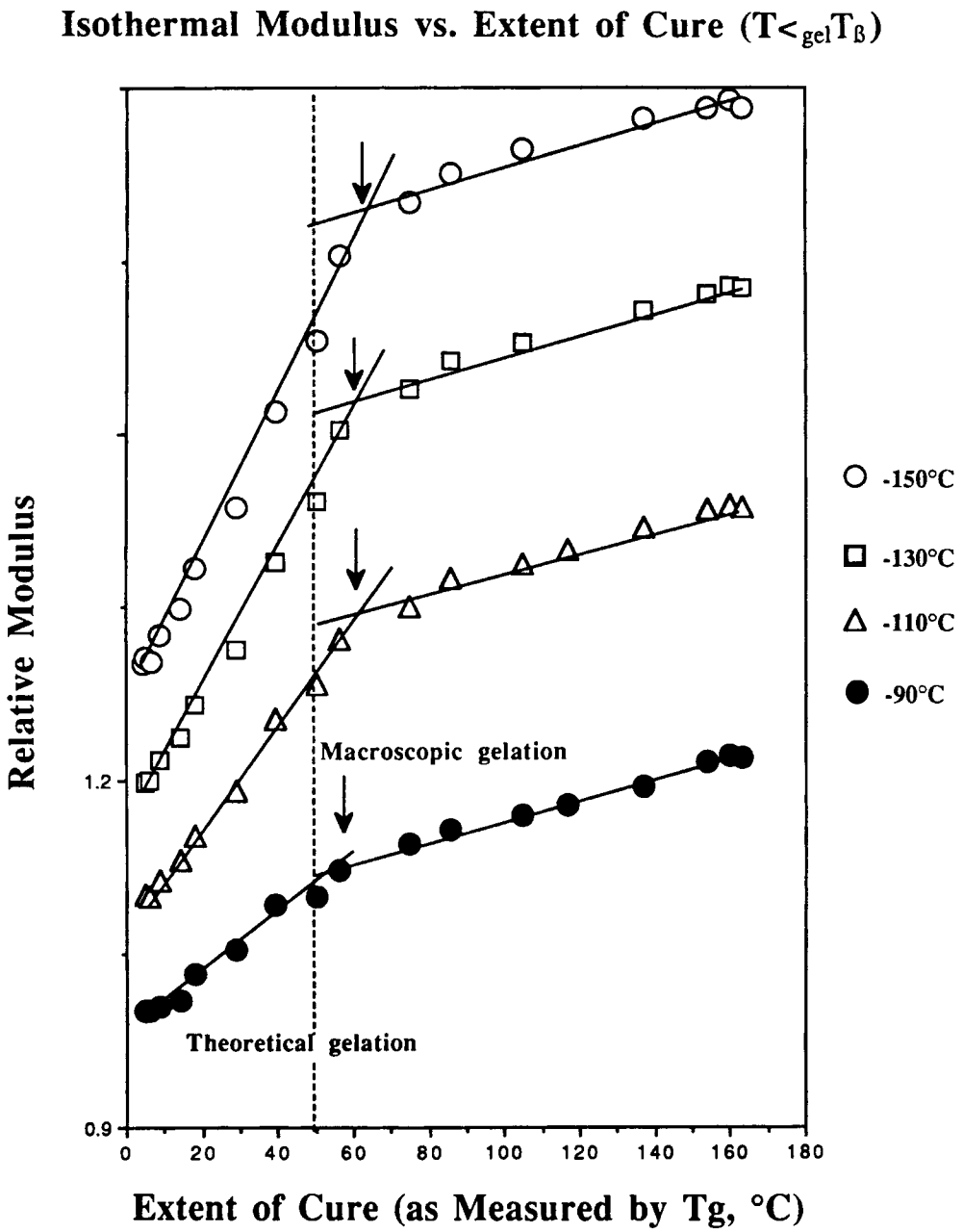

Figure 9 Isothermal relative modulus vs. extent of cure for $T < {}_{gel}T_\beta(-75°C)$. (Data for different temperatures are shifted vertically by different amounts: the relative modulus at each temperature = 1 for extent of cure = 0.) ${}_{gel}T_\beta$ is the β-transition temperature of the curing system at its theoretical gelation point. The theoretical gelation value for both T_g and T_β are evaluated from Flory's theory[26,27] and the T_g/conversion[1,2] and the T_β/T_g experimental relationships.

$-70°C \cdots$). Data were obtained during the cooling to provide T_g values. The specimen was then held at the aging temperature for more than 1000 min, during which the physical aging was monitored by measuring the increasing relative modulus [data were collected after 40 min when isothermal conditions (i.e., $T = T \pm 0.1°C$) had been established]. After aging, the specimen was heated at 1°C/min through the glass transition to about 50°C above T_g to eliminate the effects of physical aging and also to permit further cure. The specimen was then quenched again at 5°C/min through the glass transition to the same isothermal aging temperature to monitor the physical aging process for the increased

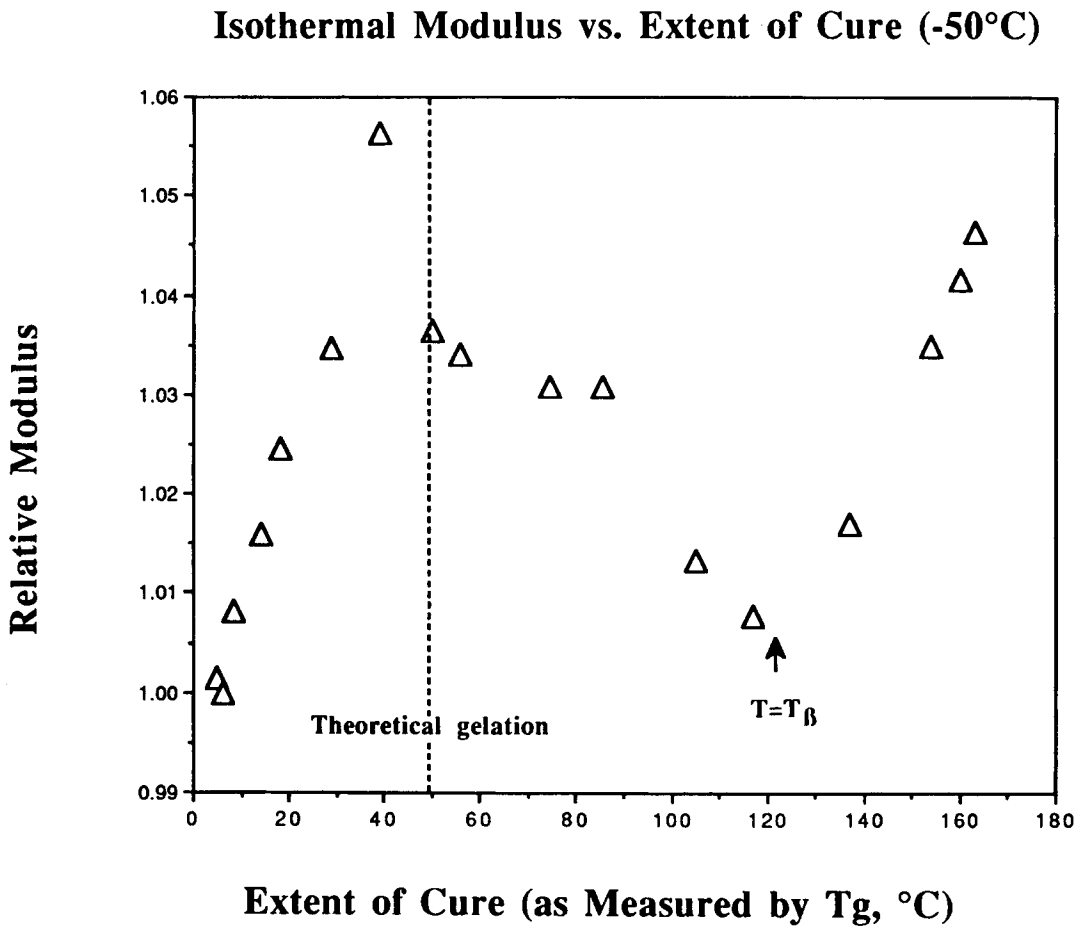

Figure 10 Isothermal relative modulus (−50°C) vs. extent of cure. The theoretical gelation value for T_g is evaluated from Flory's theory[26,27] and the T_g/conversion experimental relationship.[1,2]

conversion. The procedure was repeated 8 to 10 times for each aging temperature until the specimen was fully cured. A new specimen was used for each isothermal aging temperature vs. extent of cure experiment.

It is noted that the preaged T_g assignments at 5°C/min cooling rate were systematically different (~ 2°C) from those obtained at 1.5°C/min.

RESULTS AND DISCUSSION

T_g vs. Conversion

The preaged glass transition temperature, T_g, has been found to be a good index for monitoring chemical conversion,[1,2] since there is a one-to-one relationship between T_g and conversion (Fig. 3). The reported data of Figure 3 were obtained using the DSC technique.[1,2] The fact that T_g increases nonlinearly with conversion in crosslinking systems is considered to arise from the dependence of T_g on the crosslinking density (which is considered to be made up of tri-functional crosslinking units) and on the number average molecular weight.[1,2,5] Both experimental and theoretical analysis of the thermosetting system used in this work imply that the T_g vs. conversion relationship is unique, regardless of the chemical kinetics or the time–temperature cure path.[5,24] This is important since T_g is easily measured, sensitive to conversion with sensitivity increasing with increasing conversion, and directly relevant to the thermomechanical behavior of the material. Consequently, in the experiments reported here, the preaged T_g was used to monitor chemical conversion (hereafter designated T_g rather than "preaged T_g").

T_g and T_β

A temperature scan of the material from the liquid or rubbery state into the glassy state yields the tem-

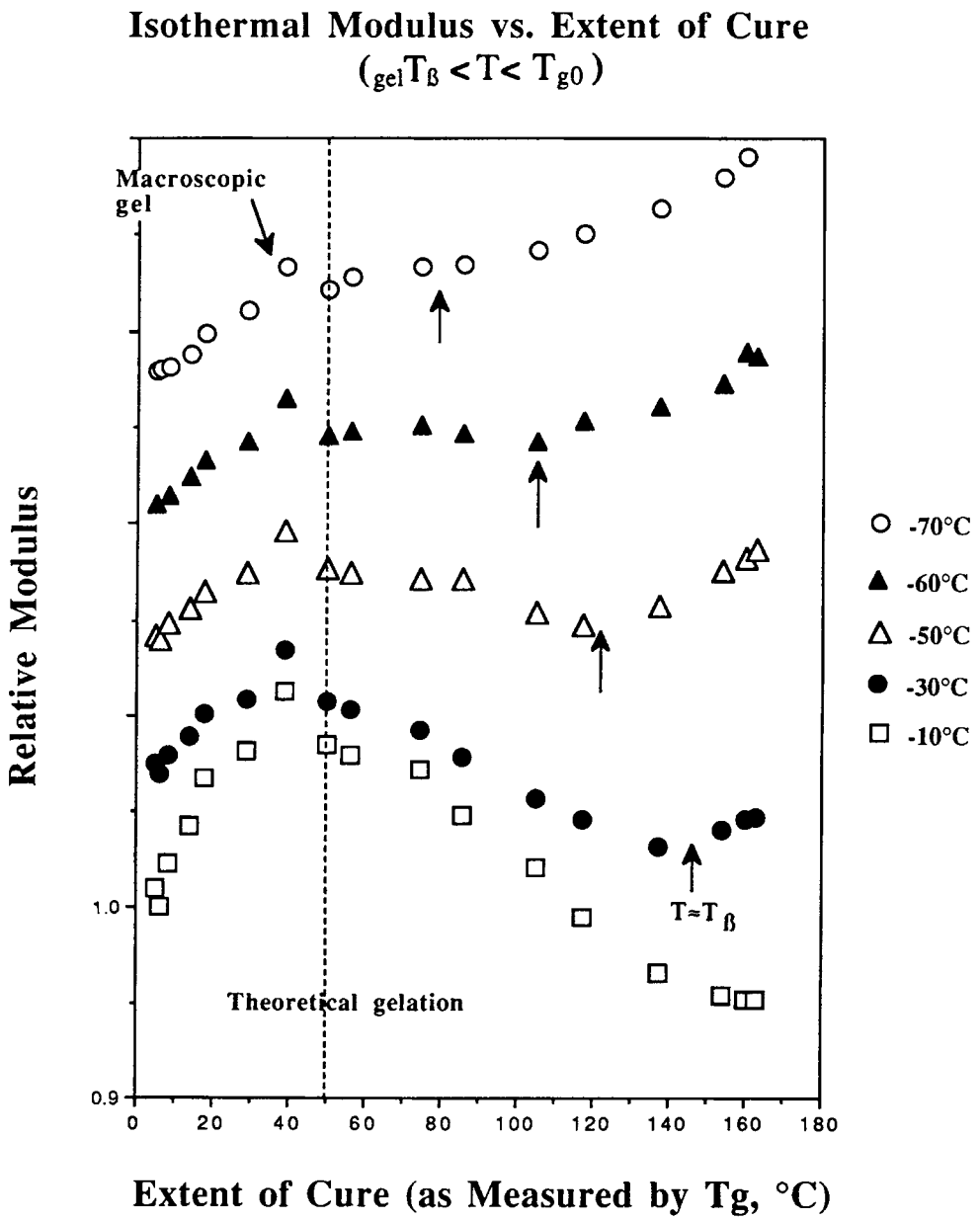

Figure 11 Isothermal relative modulus vs. extent of cure for $_{gel}T_\beta(-75°C) < T < T_{g0}(0°C)$. The theoretical gelation value for both T_g and T_β are evaluated from Flory's theory[26,27] and the T_g/conversion[1,2] and the T_β/T_g experimental relationships. (See caption for Fig. 9 with respect to vertical shifts of data.)

peratures of the glass transition (T_g) and secondary transition (T_β), as determined from the maxima in the logarithmic decrement. T_g and T_β of the curing system increase with extent of cure throughout cure (Fig. 4). T_β vs. conversion (T_g) displays a jump in the vicinity of gelation; this may be the consequence of the micromechanism of the β-transition before gelation being different from that after gelation. T_β increases linearly with T_g after the gelation point (Fig. 5). It appears that the changes of T_β and T_g are affected by similar structural factors, i.e., the crosslinking sites, after gelation.[6] The β-transition temperature of the curing system at its gelation point, defined here as $_{gel}T_\beta$, is $-75°C$. Like the corresponding glass transition temperature of the curing system at its gelation point, $_{gel}T_g(50°C)$,[25] $_{gel}T_\beta$ is a material parameter of a curing system in which gelation occurs at a definite conversion (Flory's theory), independent of the cure temperature.[26,27] The increase of T_β after the gel point, with increased

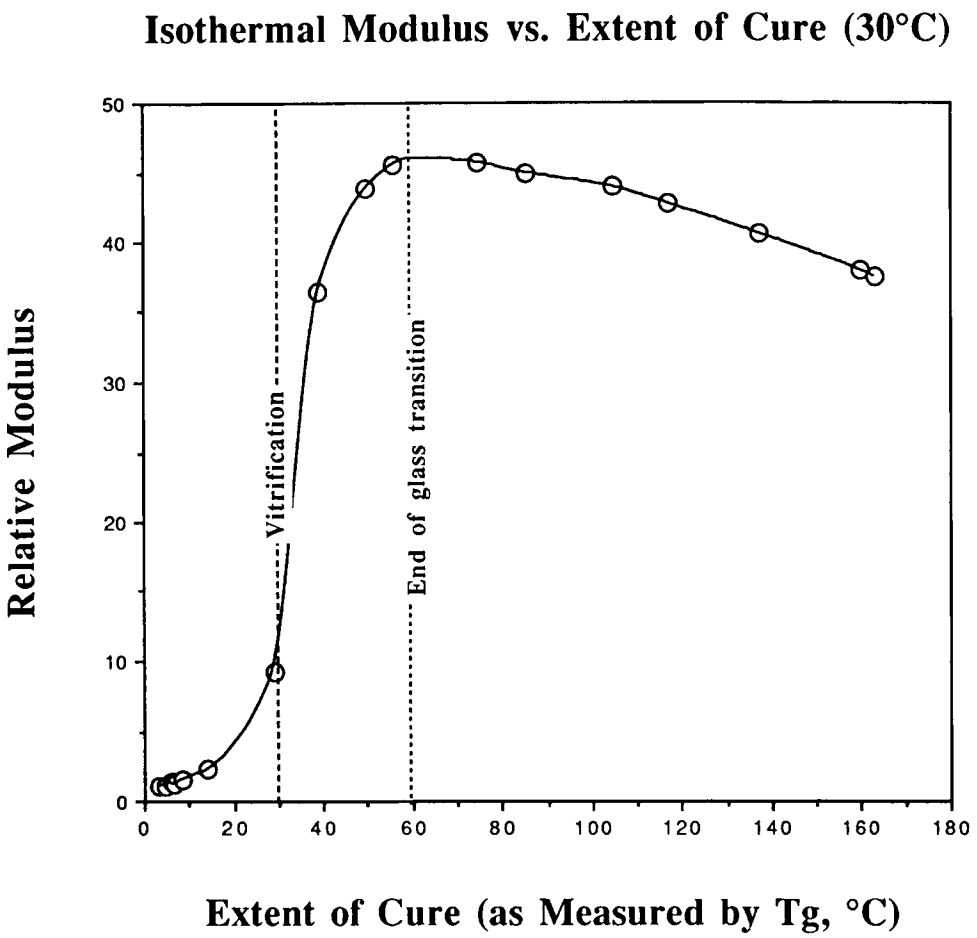

Figure 12 Isothermal relative modulus (30°C) vs. extent of cure. The vitrification value is defined as $T_g = T$. The value of end of glass transition is obtained from the maximum of the isothermal modulus vs. extent of cure.

extent of cure, significantly affects the glassy state physical properties of the curing system deep in the glassy state, as will be discussed.

Isothermal Modulus, Density, and Water Absorption

The moisture absorption behavior vs. extent of cure depends on the presence of appropriately sized "holes," which are related to the free volume (or specific volume, or density) of the material.[20] Figure 6 shows that the density at 25°C decreases, and the water absorption at 25°C increases as the extent of cure increases (after gelation). The density is inversely related to water absorption.[7,10,20,22] It is observed that postcuring an epoxy resin yields another interesting result: the glass transition temperature (T_g) increases, whereas the modulus at 25°C decreases.[6,20] The inverse relationship between the relative modulus and specific volume at 25°C is presented in Figure 7. These results show that the basic physical properties of the glassy state are related to one another and all change anomalously with increase of the extent of cure. Therefore, investigation of changes of the modulus vs. extent of cure can be used to predict corresponding changes in other properties.

Isothermal Modulus vs. Extent of Cure for $T < {}_{gel}T_\beta$ (−75°C)

The modulus of the curing system at temperatures below ${}_{gel}T_\beta$ ($\simeq -75$°C) increases linearly and sharply with an increase in the extent of cure (as measured by T_g) until the vicinity of gelation (Fig. 8). The relationship remains linear thereafter, but with a decreased slope. The results for different temperatures below ${}_{gel}T_\beta$ show (Fig. 9) that the critical point at which the modulus changes slope, which is designated macroscopic gelation on account of the macroscopic modulus changing slope in the prox-

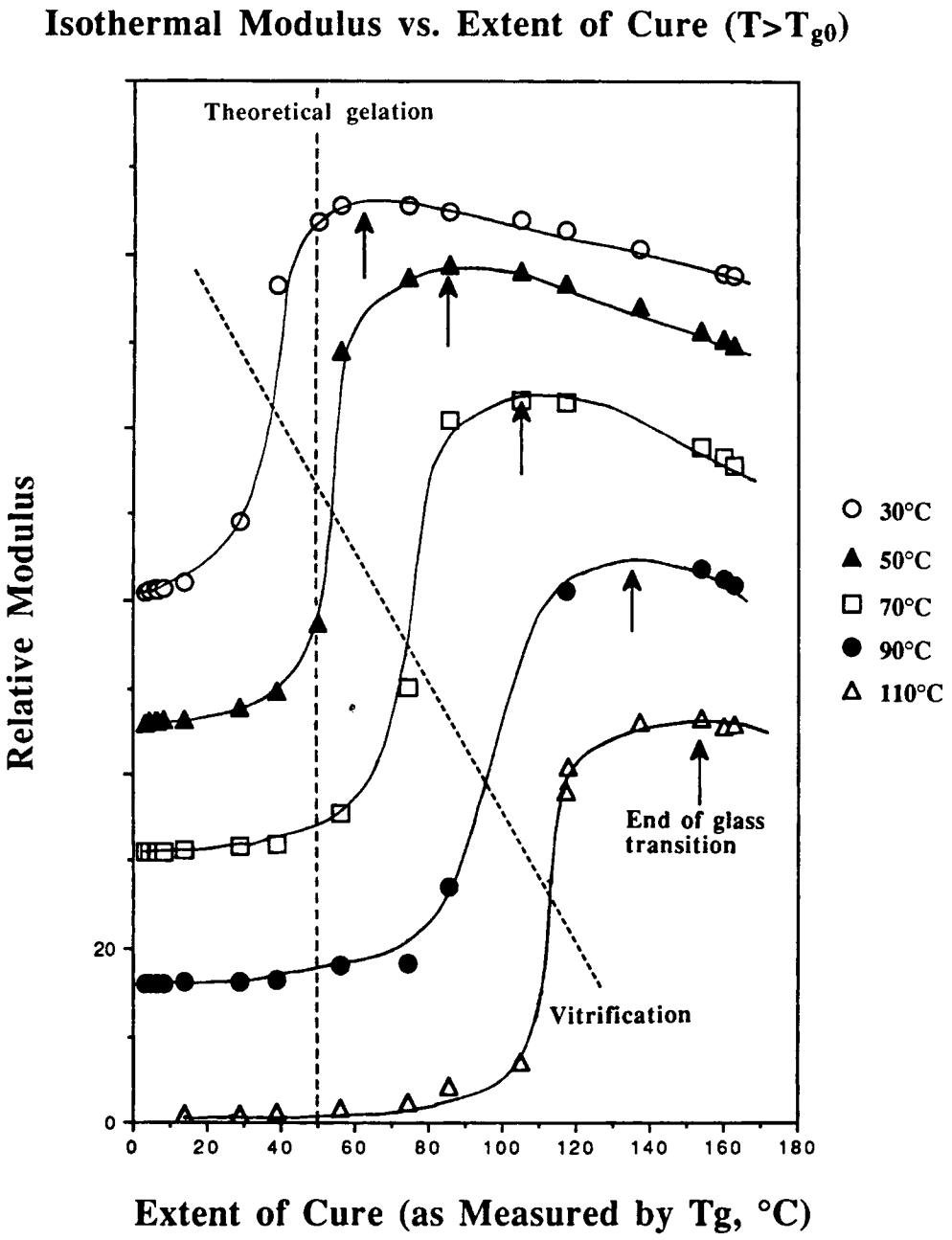

Figure 13 Isothermal relative modulus vs. extent of cure for $T > T_{g0}(0°C)$. The arrows indicate the vicinity of the end of glass transition. (See caption for Fig. 9 with respect to vertical shifts of data.)

imity of the theoretical gelation point, is not sensitive to temperature over a wide temperature range below temperature ${}_{gel}T_{\beta}$.

Isothermal Modulus vs. Extent of Cure for ${}_{gel}T_{\beta}$ ($-75°C$) < T < T_{g0} (0°C)

The modulus vs. extent of cure (as measured by T_g) for temperatures between ${}_{gel}T_{\beta}$ and T_{g0} (-75 to 0°C) is a source of surprise; for example, at the temperature $T = -50°C$ (Fig. 10), which is always deep in the glassy state, the relative modulus increases rapidly reaching a maximum when the T_g of the material $\simeq$ 40°C, then decreases to a minimum when the T_g of the material $\simeq$ 120°C, after which it increases again with increase of the extent of cure. There is no significant influence of temperature on the extent of cure at the maximum (Fig. 11), which is designated macroscopic gelation on account of its prox-

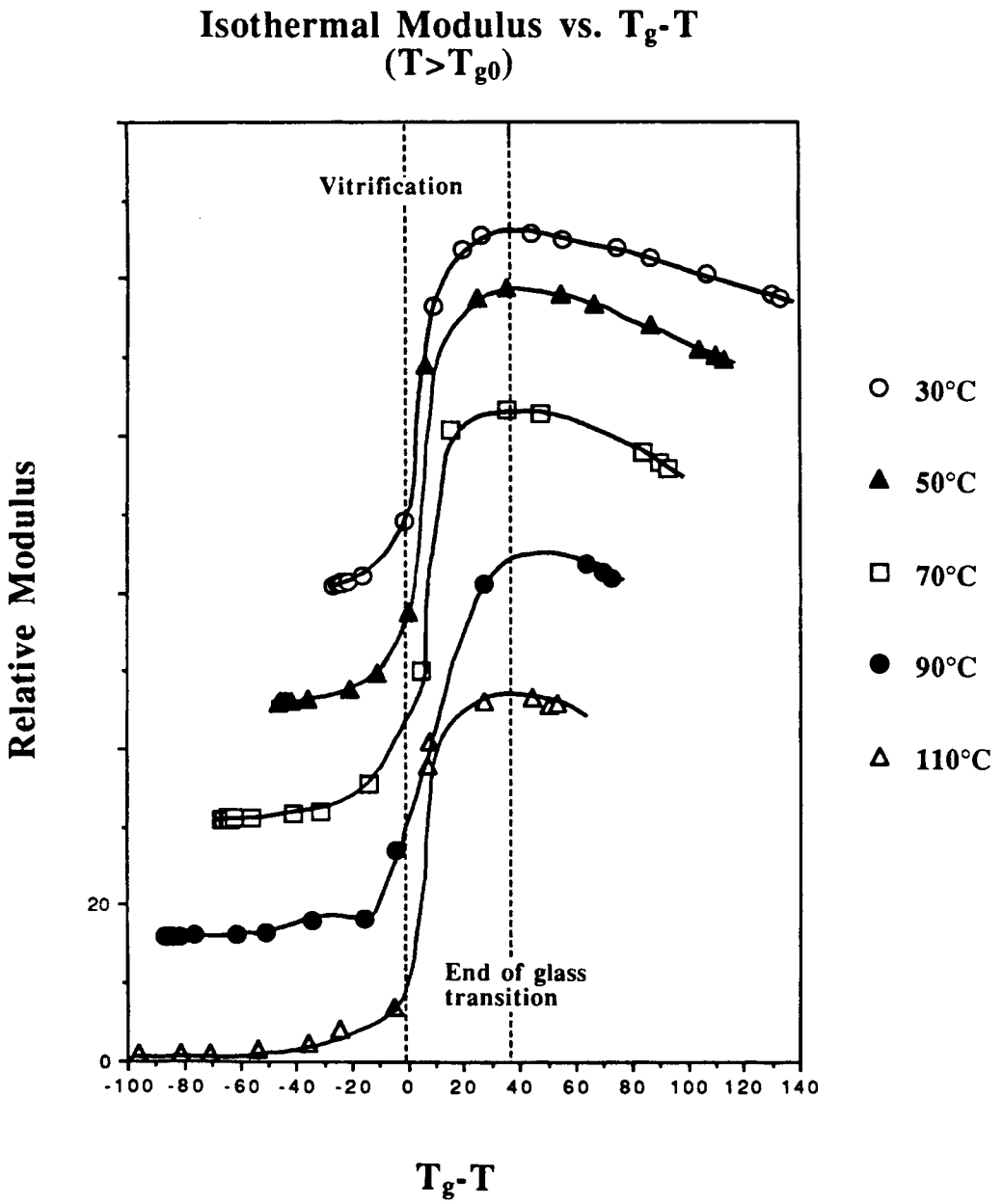

Figure 14 Relative modulus vs. T_g–T. Experimental data of Figure 13 replotted using T_g–T as the X-axis.

imity to the theoretical gelation point.[1,2,26,27] The modulus of the curing system before and after gelation behave inversely. After gelation, the modulus decreases with increasing cure until reaching a minimum. The extent of cure at the minimum increases with temperature. Correlation with experimental data shows that the minimum is related to the conversion at which T_β rises through the temperature of measurement (Fig. 11). It is noteworthy that the modulus again behaves inversely before and after this minimum with respect to increasing cure.

Isothermal Modulus vs. Extent of Cure for $T > T_{g0}$ (0°C)

The material is initially in the liquid state when temperature $T > T_{g0}$. Figure 12 shows that the relative modulus of the material at T = 30°C rises through vitrification ($T_g = T$), reaches a maximum beyond vitrification, and then decreases with increasing extent of cure.

However, the maximum in the relative modulus vs. conversion is not related to the gelation point,

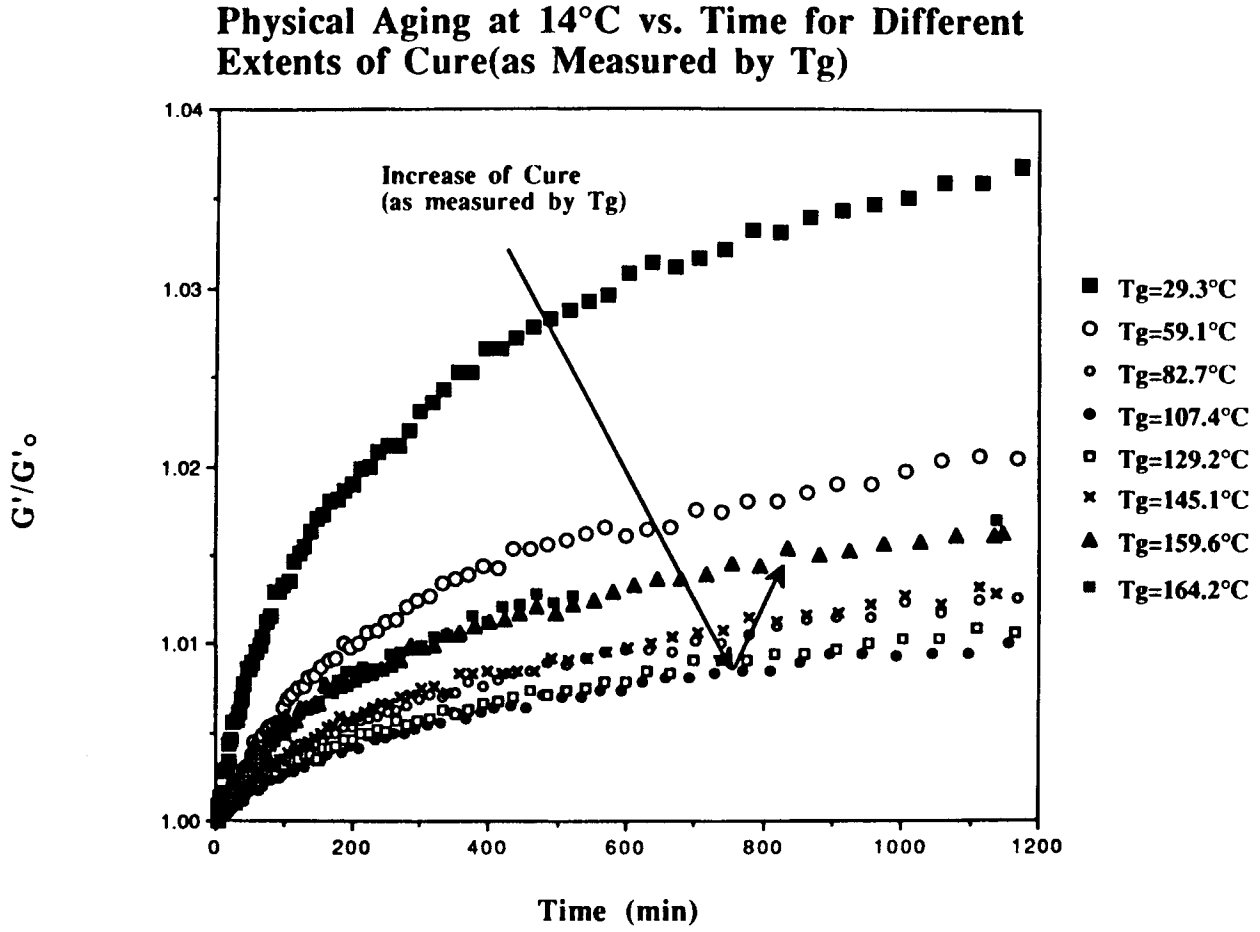

Figure 15 Isothermal relative modulus at 14°C vs. aging time for different extents of cure, after cooling from above T_g at 5°C/min to 14°C. The rate of aging decreases and then increases with increasing of extent of cure (see arrows).

which is in contradiction to previous reports.[18,19] Experimental results show that the extent of cure at the maximum increases with an increase in the isothermal temperature (Fig. 13). On using T_g–T as the X-axis to replot the experimental data of Figure 13, the relative modulus vs. extent of cure at different temperatures shows the same shape with the same maximum at T_g–$T \simeq 35$°C (Fig. 14). The maximum in the isothermal modulus vs. extent of cure is related to the end of the glass transition region, which therefore is defined as the end of glass transition of the curing system, ${}_eT_g$, (${}_eT_g \simeq T_g - 35$°C).

Isothermal Physical Aging Rate vs. Extent of Cure for $T_\beta < T < T_g$

The isothermal relative modulus of the partially cured material, after cooling from above T_g at 5°C/min to a specific aging temperature (T) below T_g, increases with aging time (t_a), for example, as presented in Figure 15, for different extents of cure for isothermal temperature T = 14°C. The increase of modulus is related to the spontaneous reduction in the excess volume, which is trapped in the glassy state during cooling. Many studies, including small strain creep, stress relaxation, modulus, enthalpy relaxation, volume relaxation, and dielectric relaxation[28-33] experiments, have shown that physical aging at long times is linear with respect to logarithm aging time. Figure 16 shows that the increase of the modulus of the undercured material deep in the glassy state is linear with the logarithm of t_a at long times.

The aging rate is defined as

$$R_a(T) = [d(G'/G'_0)/d(\log t_a)]$$

where G'_0 is the initial modulus of the material at the beginning (after 40 min when isothermal conditions had been established) of isothermal aging. Aging rate vs. extent of cure results for different

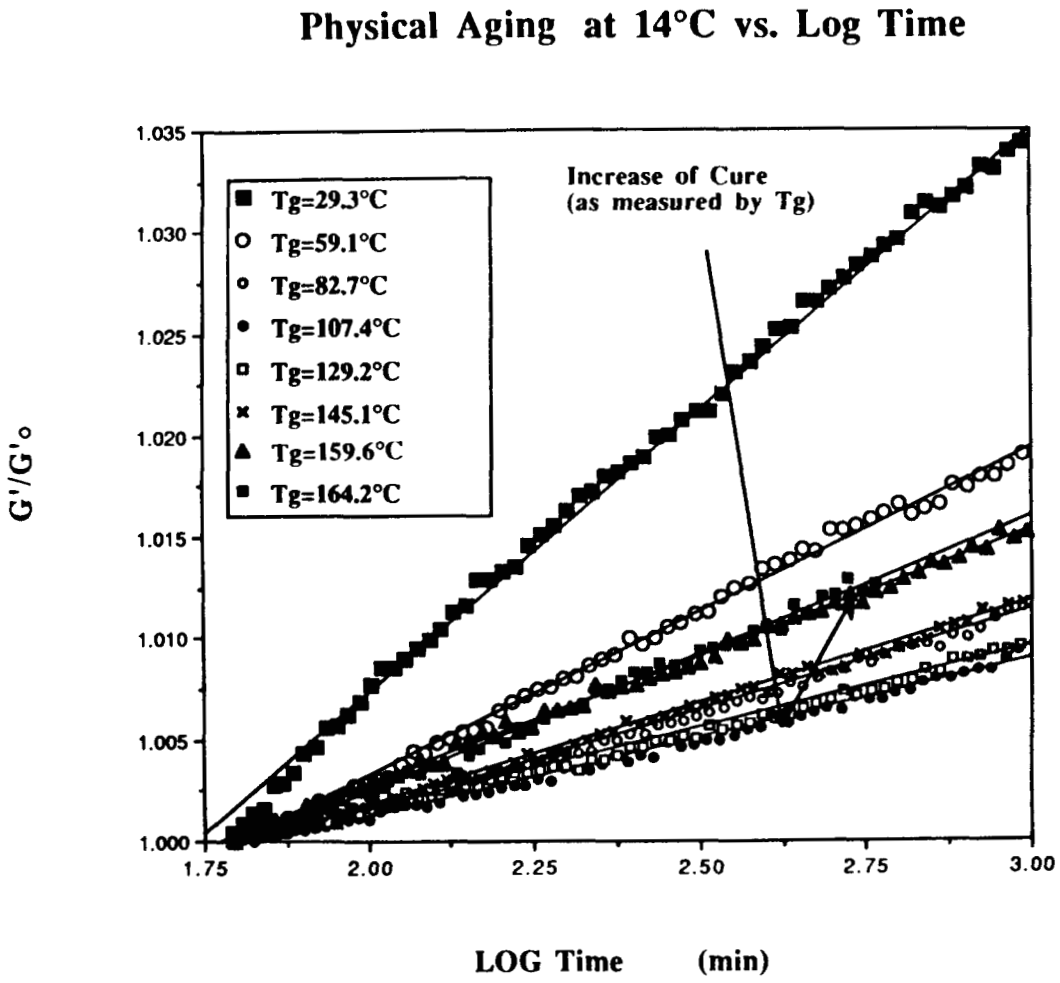

Figure 16 Physical aging rate at 14°C vs. logarithm time for different extents of cure. Physical aging at long times is linear with respect to logarithm aging time.

isothermal temperatures are presented in Figure 17. The physical aging rate, $R_a(T)$, of this material at given isothermal aging temperatures (i.e., $T = -35.5$, -15, 14, 45°C) decreases with increase of extent of cure until reaching a minimum, after which $R_a(T)$ increases again with further increase of extent of cure. This anomaly is considered to be the consequence of the dynamic thermomechanical logarithmic decrement spectrum, which shows a minimum between T_g and T_β.[33] The extent of cure at the minimum increases with aging temperature. However, on using T_g-T as the X-axis to replot the experimental data of Figure 17, the aging rates at different temperatures vs. extent of cure show the same shape with the same minimum at $T_g-T \simeq 100$°C (Fig. 18). As the interval from the equilibrium state increases, as measured by T_g-T, the physical aging rate initially decreases, but then increases for $T_g-T > 100$°C until $T_g-T \simeq T_g-T_\beta$. Interestingly, all curves may be simply vertically shifted together, as shown in Figure 19, which shows that the physical aging process of this material at a given temperature, T, is mainly governed by the departure of the material from its equilibrium state (as measured by T_g-T), regardless of chemical structure.[33] The vertical shift factor is a function of aging temperature, which follows a restricted form of the Arrhenius equation with an activation energy = 3 kcal/mol.[33]

T_g–Temperature Property (T_gTP) Diagram

The above results can be summarized in the form of the T_g–Temperature Property (T_gTP) Diagram (Fig. 20), which shows that the basic properties of the curing system may be separated into different regions by the different transition lines, i.e., gelation ($_{gel}T_g$), and the glass transition (T_g), the end of the glass transition ($_eT_g \approx T_g - 35$°C) and the β-transition (T_β) vs. extent of cure.

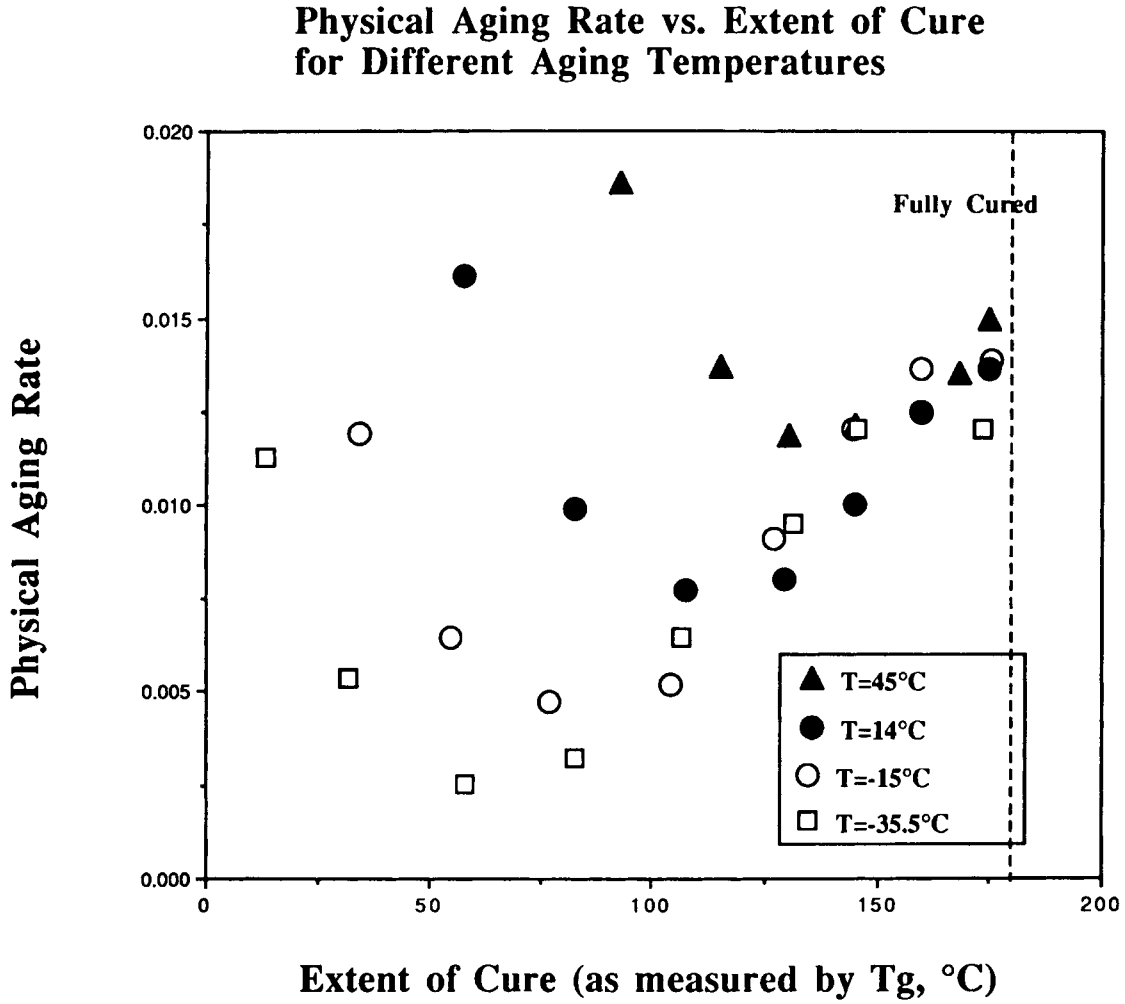

Figure 17 Physical aging rate vs. extent of cure for different isothermal temperatures.

1. Ungelled glass region, $T < {}_eT_g$ and $T_{g0} < T_g < {}_{gel}T_g$: the isothermal modulus of the material increases linearly and sharply with increase of extent of cure.
2. Gelled glass region *I*, $T_\beta < T < {}_eT_g$ and ${}_{gel}T_g < T_g < T_{g\infty}$: the isothermal modulus of the material decreases with increase of extent of cure. The isothermal physical aging rate passes through a minimum with increase of extent of cure; the minimum is related to the T_g and T_β transitions.[33]
3. Gelled glass region II, $T < T_\beta$ and ${}_{gel}T_g < T_g < T_{g\infty}$: the isothermal modulus of the material increases at a low rate with increase of extent of cure relative to that in the ungelled glass region.
4. Glass transition region, ${}_eT_g < T < T_g + 20°C$ and $T_{g0} < T_g < T_{g\infty}$: the modulus of the material shows a large progressive increase with increase of extent of cure because of vitrification, attaining a maximum at ${}_eT_g$ beyond vitrification. The glass transition region includes three lines in the T_gTP diagram; i.e., onset of glass transition ($\approx T_g + 20°C$), vitrification (T_g), and end of glass transition (${}_eT_g \approx T_g - 35°C$).
5. Sol fluid region, $T > T_g$ and $T_{g0} < T_g < {}_{gel}T_g$: the material is a viscous fluid with low modulus. The modulus shows a small step-increase near the gel point with increase of extent of cure.[6]
6. Sol-gel rubber region, $T > T_g$ and ${}_{gel}T_g < T_g < T_{g\infty}$: the modulus increases with increase of extent of cure.

The anomalous behavior of isothermal modulus and isothermal physical aging rate of the system vs. extent of cure implies that all basic physical properties display anomalous isothermal changes with an increase in extent of cure. The anomalous behavior at different temperatures depends on gelation and on the conversions at which T_g and T_β of the

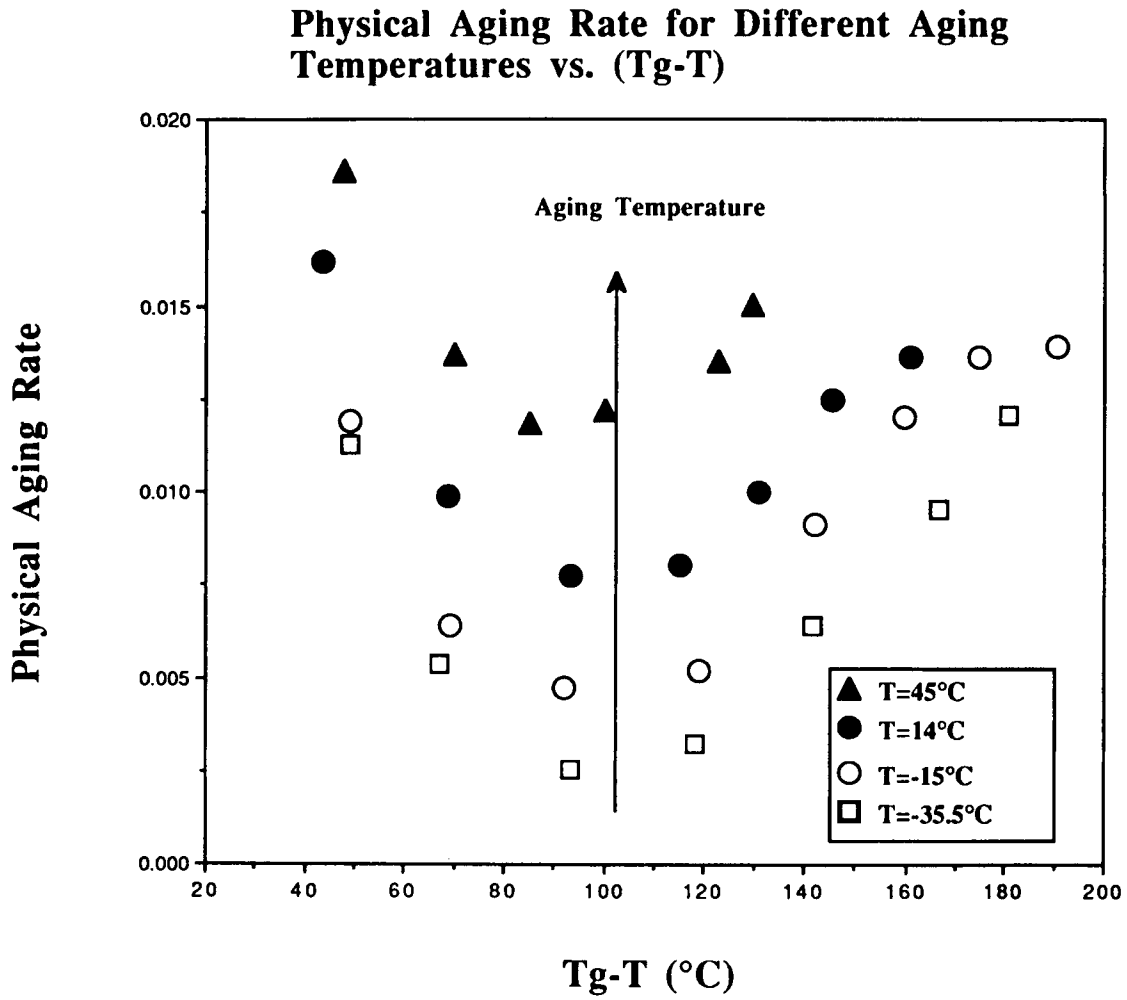

Figure 18 Physical aging rate vs. T_g–T. Experimental data of Figure 17 replotted using T_g–T as the X-axis.

material meet the temperature of the material. The changes of properties at different temperatures vs. extent of cure are summarized in the form of the T_gTP Diagram.

The significance of the T_gTP diagram is that the critical points (such as the maximum and minimum of modulus, and the minimum of the physical aging rate, vs. extent of cure) are linear or parallel to the vitrification (T_g) line; that is, the properties of thermosetting materials in the glassy state are mostly determined by the interval T_g–T of the material from the glass transition temperature. For example, it appears that there is a superposition principle for normalizing the physical aging behavior of thermosetting glasses, which involves a shift of T_g–T (i.e., a measure of departure from the equilibrium state) and a shift of $f(T)$ (i.e., a function of measurement temperature). Use of T_g as a measure of extent of cure (rather than conversion) results in linearization of relationships between the critical points and temperature in the T_gTP Diagram. This facilitates construction of T_gTP Diagrams for different systems. These simple diagrams are intellectually useful for understanding the changes of properties of materials vs. extent of cure for both undercured material (with change of conversion) and fully cured materials (with change of stoichiometric ratio).

The data in this article could have been presented as specific three dimensional T_g–Temperature Property diagrams, that is, the T_g–Temperature–Modulus diagram and the T_g–Temperature–Physical Aging Rate diagram. All other low-deformation properties can be similarily summarized. The T_g–Temperature Property diagram is the basis for all three dimensional specific property diagrams.

The anomalous behavior in the glassy state is not widely appreciated. Earlier work in this laboratory had correlated various physical phenomena vs. extent of cure to the anomalous behavior in density.

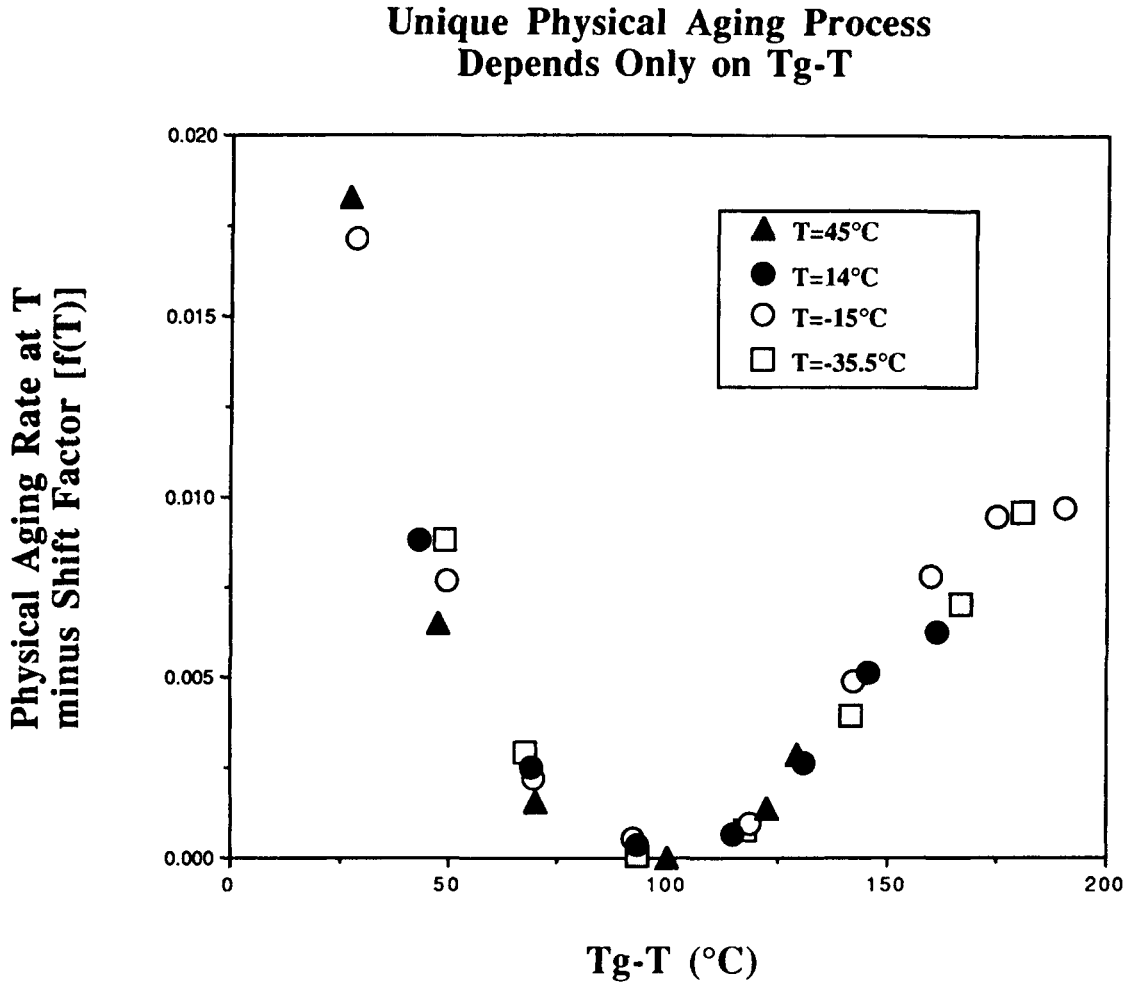

Figure 19 Unique physical aging rate vs. T_g–T. Superimposed data of Figure 17 obtained using a double shift [horizontal = T_g–T, vertical = $f(T) = A \exp(-E/RT)$].

The present work shows that the anomalous behavior in the modulus and in the physical aging rate vs. extent of cure is related to gelation and to the various transition events that occur when T_g and T_β of the material meet the temperature of the material. In future research an explanation in structural and kinetic terms will be sought. A preliminary explanation of these anomalies in the behavior of isothermal properties vs. extent of cure considers: (1) crosslinking sites occupy more volume than would be expected; this produces an influence after gelation, and (2) increase of crosslinking density and average molecular weight lead to a decrease of segmental mobility (i.e., an increase of relaxation time), which depends on T_g–T.

The T_gTP diagram is related to other cure/transformation diagrams, that is, the Time–Temperature–Transformation Cure diagram and the Conversion–Temperature–Transformation Diagram.[34] A discussion of the three diagrams is presented in the Appendix.

CONCLUSIONS

The isothermal physical properties in the glassy state of thermosetting crosslinked polymers vs. conversion are anomalous and complex. The anomalous behavior at different isothermal temperatures vs. extent of cure depends on gelation and on the events that occur when T_g and T_β of the material meet the temperature of the material. The changes of properties at different temperatures vs. extent of cure are summarized in the form of a T_g–Temperature Property (T_gTP) Diagram. An explanation is being

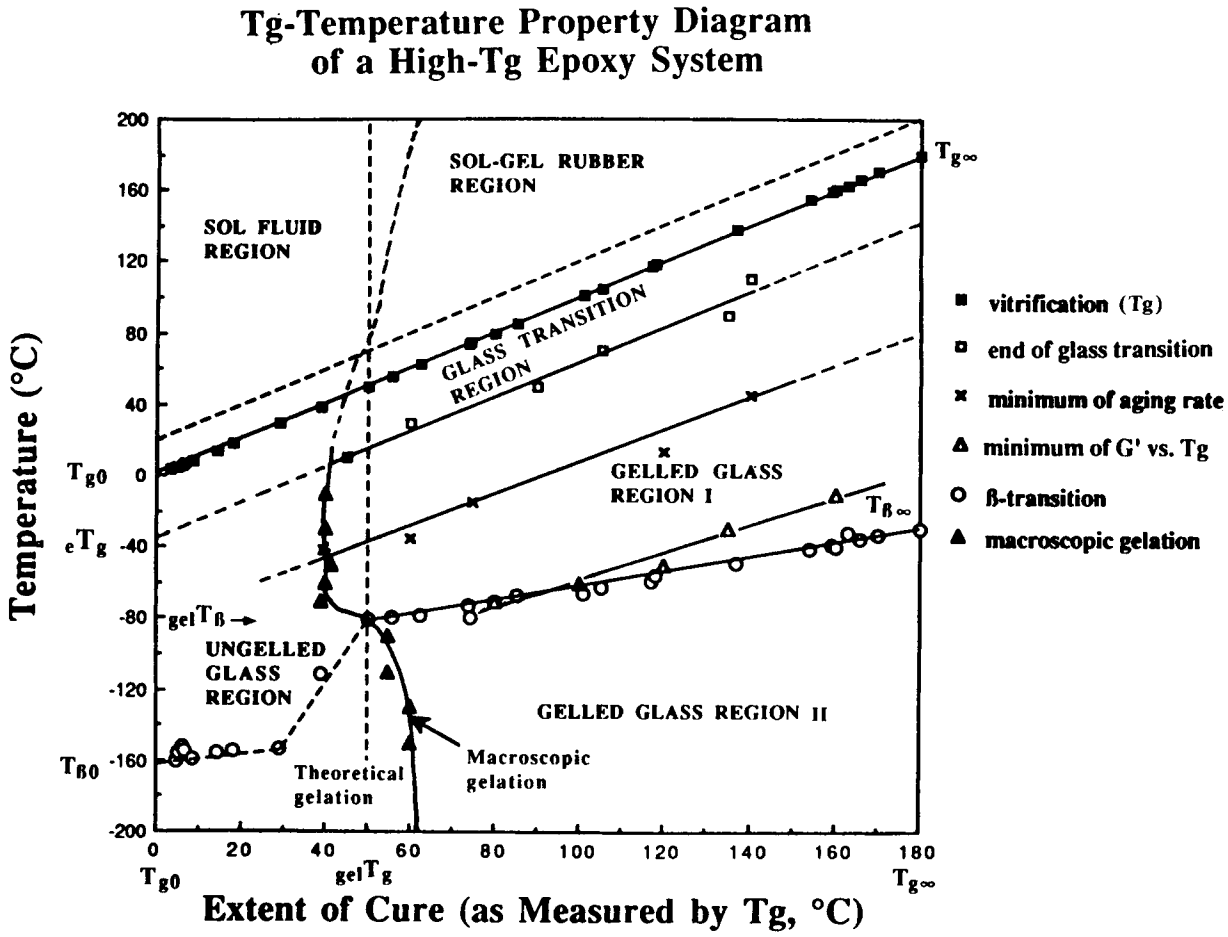

Figure 20 T_g–Temperature Property (T_gTP) Diagram. The theoretical gelation values for T_g, $_{gel}T_g$, and T_β, $_{gel}T_\beta$, are evaluated from Flory's theory[26,27] and the T_g/conversion[1,2] and the T_β/T_g experimental relationships. The marked macroscopic gelation point values are assigned from the changes of the relative modulus in the glassy state vs. extent of cure, which occur near the theoretical gelation point (see also Figs. 9 and 11).

sought on the basis of kinetic and structural contributions.

Financial support has been provided by Hercules, Inc.

APPENDIX

Cure/Property Diagrams of Thermosetting Systems

The transformation of reactive thermosetting liquid to glassy solid generally involves two distinct macroscopic transitions: macroscopic gelation and vitrification. Molecular gelation, which corresponds to the incipient formation of infinite molecules and occurs at a definite conversion for a simple system (according to Flory's theory of gelation), gives rise to long range elastic behavior in the macroscopic fluid. Vitrification occurs when the glass transition temperature (T_g) of the system rises to the cure temperature. The non-linear increase in the T_g vs. conversion relationship is made up of two effects: increase of molecular weight and increase of degree of crosslinking with increase of extent of cure. The occurrence of the two transitions during cure is the basis of the Time–Temperature–Transformation (TTT) Cure Diagram and the Conversion–Temperature–Transformation Diagram. Furthermore, physical properties deep in the glassy state (e.g., density, modulus, and physical aging rate) vs. extent of cure are determined principally by the temperature interval T_g–T and are affected by the T_g and T_β-transitions (both of which increase with increase

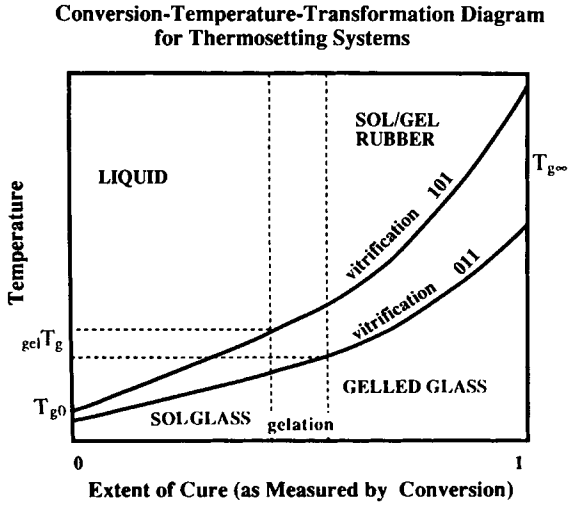

Figure 21 Conversion–Temperature–Transformation (CTT) Diagram for a thermosetting system.[39] Shown are the vitrification ($T = T_g$) vs. conversion contours for reactants with different functionality (101 > 011). The conversions at gelation are also included.

of extent of cure for the epoxy/amine thermosetting system). These latter characteristics provide the basis for the T_g–Temperature Property (T_gTP) Diagram. These diagrams are intellectual frameworks for understanding relationships between reactants, cure path, structure, transformations, material states, and properties.

Conversion–Temperature–Transformation (CTT) Diagram

The chemical conversion at molecular gelation and the contour of the reaction temperature vs. the chemical conversion at vitrification form the Conversion–Temperature Cure (CTT) Diagram[35–39] (Fig. 21). For epoxies, this diagram separates the kinetically controlled reaction region and the diffusion controlled reaction region by the nonlinear relationship between $T = T_g$ and conversion. The relationship can be used to demonstrate the effects

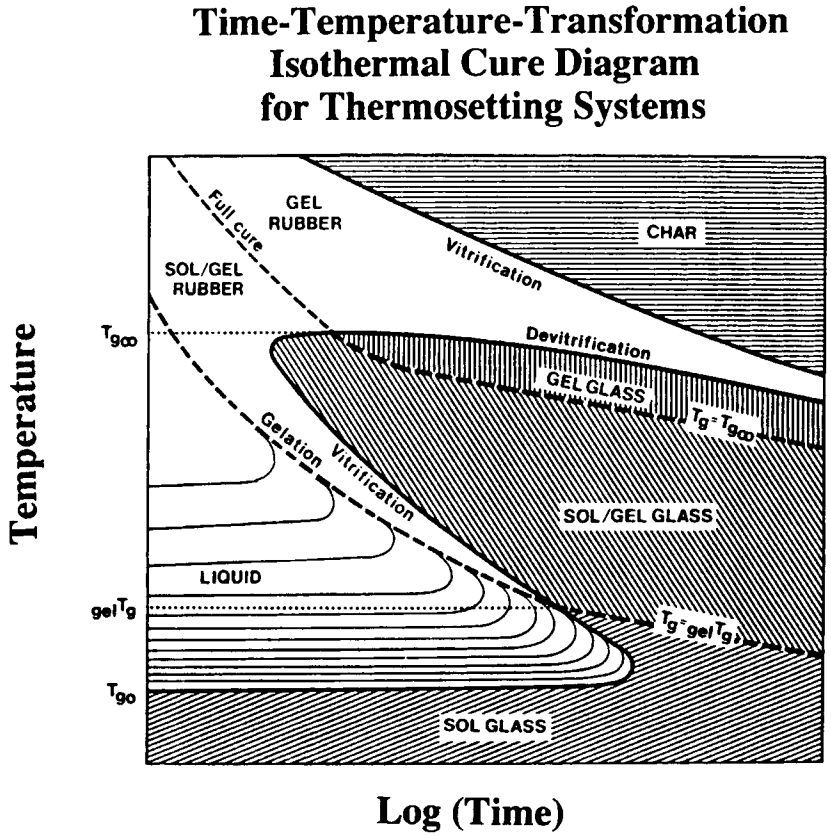

Figure 22 Time–Temperature–Transformation (TTT) isothermal cure diagram for a thermosetting system. Shown are three critical temperatures, i.e., $T_{g\infty}$, $_{gel}T_g$, T_{g0}, and the distinct states of matter, i.e., liquid, sol/gel rubber, gel rubber, sol glass, sol/gel glass, gel glass, and char. The full-cure line is $T_g = T_{g\infty}$. Devitrification is the consequence of thermal degradation at high cure temperatures. Isoviscosity contours in the liquid region are also included.

of increasing functionality of the reactants on gelation and vitrification, and also the effect of steric hinderance of the reactants and products. The key feature of the diagram is that chemical conversion is used as the X-axis.

Time–Temperature–Transformation Cure (TTT) Diagram

The contours of the time to gel and to vitrify vs. the reaction temperature form the basis of the isothermal TTT cure diagram (Fig. 22) and the corresponding continuous heating (CHT) cure diagram (Fig. 23).[6,23,40] These diagrams provide maps of different regions, which are defined by the "S" shaped vitrification curve and the nonlinear gelation curve. The choice of a particular time–temperature cure path involves consideration of the kinetically controlled reaction region (principally liquid and sol/gel rubber regions) and the diffusion controlled reaction region (principally sol glass and sol/gel glass regions). The technological terms, *A*-, *B*-, and *C*-stage resins correspond to sol glass, sol/gel glass, and fully cured gel glass regions in the diagrams. The key feature of the diagrams is that log (time) is used as the X-axis.

T_g–Temperature Property (T_gTP) Diagram[42]

The relationships of the contours of the glass transition (T_g) and the β-transition (T_β) (both of which increase with increase of extent of cure) to the material temperature is the basis of the T_g–Temperature Property (T_gTP) Diagram (Fig. 1). The diagram provides a methodology for understanding the anomalous and complex relationships between basic physical properties (such as density and modulus) in the glassy state of thermosetting systems and conversion.[6–22,41] The properties behave differently with respect to increasing extent of cure before gelation and after gelation in both the glassy region and the liquid/rubber region. Furthermore, the other critical points, at which isothermal properties vs. extent of cure change anomalously, are linear or parallel to the vitrification (T_g) and β-transition lines. Anomalies in isothermal behavior occur when the material passes through adjacent regions with increased extent of cure. The diagram can be used to investigate the physical properties of both undercured material (with change of conversion) and fully cured materials (with change of stoichiometric ratio). The key feature of the diagram is that T_g is used as the X-axis, which results in linearization of the conversion–temperature property, T_gTP, diagram.

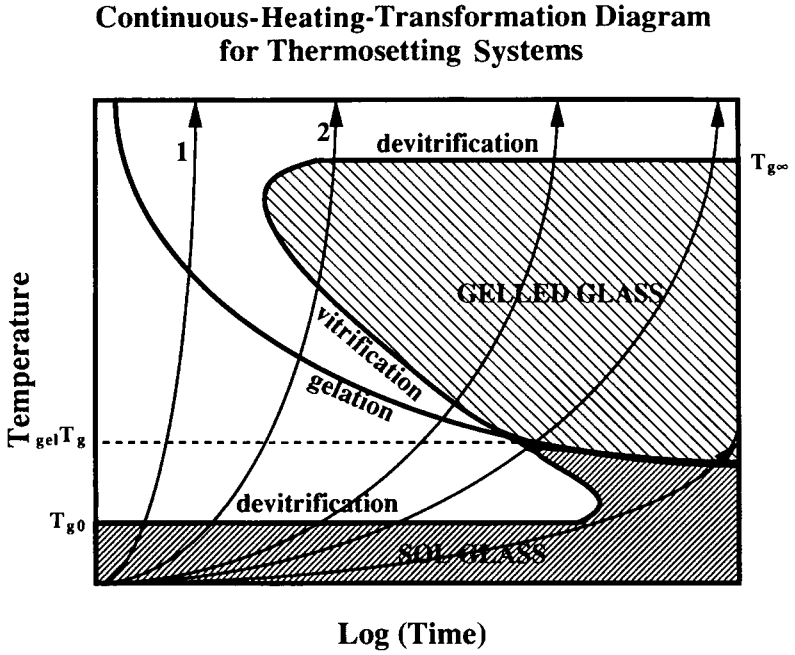

Figure 23 Continuous–Heating–Transformation (CHT) diagram for a thermosetting system. Included are the initial devitrification, vitrification, and upper devitrification events, which are determined from the intersections of the temperature/time and T_g/time curves at different heating rates. Continuous heating cure paths (i.e., rate 1 > rate 2) are also included (see arrows).

The Y-axis presents temperature in the diagrams; whereas, the X-axis presents extent of cure in terms of log (time) in the TTT and the CHT cure diagrams, chemical conversion in the CTT diagram, and T_g in the T_gTP diagram, respectively. The diagrams are interrelated by reaction kinetics, conversion/T_g and property/T_g relationships. The CTT diagram and the TTT and the CHT diagrams are useful for investigating the extreme rheological changes of thermosetting systems during cure. The T_gTP diagram is useful for understanding the physical properties of a cured glassy material with change of extent of cure or with change of stoichiometric ratio.

REFERENCES

1. G. Wisanrakkit and J. K. Gillham, *J. Coat. Tech.*, **62**(783), 35 (1990).
2. G. Wisanrakkit and J. K. Gillham, *J. Appl. Polym. Sci.*, **41**, 2885 (1990).
3. S. L. Simon and J. K. Gillham, *ACS Polym. Mat. Sci. Eng. Div. Prepr.*, **61**, 799 (1989). Also: *J. Appl. Polym. Sci.*, **46**, 1245 (1992).
4. S. L. Simon, J. K. Gillham and D. A. Shimp, *ACS Polym. Mat. Sci. Eng. Div. Prepr.*, **62**, 96 (1990).
5. X. Wang and J. K. Gillham, *J. Appl. Polym. Sci.*, **45**, 2127 (1992).
6. J. B. Enns and J. K. Gillham, *J. Appl. Polym. Sci.*, **28**, 2831 (1983).
7. J. P. Aherne, J. B. Enns, M. J. Doyle, and J. K. Gillham, *ACS Org. Coat. Plast. Chem. Div. Prepr.*, **46**, 574 (1982).
8. M. T. Aronhime, X. Peng, J. K. Gillham, and R. D. Small, *J. Appl. Polym. Sci.*, **32**, 3589 (1986).
9. S. Mostovoy and E. J. Ripling, *J. Appl. Polym. Sci.*, **10**, 1351 (1966).
10. V. B. Gupta and L. T. Drzal, *J. Appl. Polym. Sci.*, **30**, 4467 (1985).
11. A. Shimazaki, *J. Polym. Sci. Part C*, **23**, 555 (1968).
12. M. Cizmecioglu, A. Gupta, and F. R. Fedors, *J. Appl. Polym. Sci.* **32**, 6177 (1986).
13. W. Fisch, W. Hofmann, and R. Schmid, *J. Appl. Polym. Sci.*, **13**, 295 (1969).
14. W. Fisch and W. Hofmann, *Plast. Tech.*, Aug., 1966, pp. 28–32.
15. N. Shito, *J. Polym. Sci. Part C*, **23**, 569 (1968).
16. S. K. Dirlikov, *High Perform. Polym.*, **2**, 61 (1990).
17. S. L. Simon and J. K. Gillham, *ACS Div. Polym. Chem.*, **32**(2), 812–184 (1991); *Polym. Tech. Confer.*, Philadelphia, PA., June 3–5, 1991. Also: *J. Appl. Polym. Sci.*, to appear (1992).
18. D. A. Shimp, *ACS Polym. Mat. Sci. Eng. Div. Prepr.*, **54**, 107 (1986).
19. K. P. Pang and J. K. Gillham, *J. Appl. Polym. Sci.*, **37**, 1969 (1989).
20. M. T. Aronhime, X. Peng, and J. K. Gillham, *J. Appl. Polym. Sci.*, **32**, 3589 (1986).
21. M. A. Taylor and J. K. Gillham, *ACS Polym. Mat. Sci. Eng. Div. Prepr.*, **61**, 806 (1989).
22. Y. G. Won, J. Galy, and J. P. Pascault, *Polymer*, **32**, 79 (1991).
23. J. K. Gillham in Developments in Polymer Characterisation, Vol. 3, Chap. 5, J. V. Dawkins, Ed., Applied Science, London, 1982, pp. 159–227.
24. X. Wang and J. K. Gillham, *ACS Polym. Mat. Sci. Eng. Div. Prepr.*, **63**, 505 (1990).
25. P. G. Babayevsky and J. K. Gillham, *J. Appl. Polym. Sci.*, **17**, 2067 (1973).
26. P. J. Flory, Principles of Polymer Chemistry, Cornell University Press, New York, 1953, p. 432.
27. D. R. Miller and C. W. Macosko, *Macromolecules*, **9**, 206 (1976).
28. G. Wisanrakkit and J. K. Gillham, *J. Appl. Polym. Sci.*, **42**, 2465 (1991).
29. S. Matsuoka, *Polym. Eng. Sci.*, **18**, 1073 (1978).
30. Z. H. Ophir, J. A. Emerson, and G. L. Wilkes, *J. Appl. Phys.*, **49**(10), 5032 (1978).
31. K. C. Rusch, *J. Macromol. Sci. Phys.*, **B2**(2), 179 (1968).
32. M. Uchidoi, K. Adachi, and Y. Ishida, *Polym. J.*, **10**, 161 (1978).
33. X. Wang and J. K. Gillham, *Soc. Plast. Eng. Prepr. Ann. Tech. Conference*, Montreal, Canada, 1991, pp. 732–736. Also: *J. Appl. Polym. Sci.*, **47**, 447 (1993).
34. X. Wang and J. K. Gillham, *ACS Polym. Mat. Sci. Eng. Div. Prepr.*, **65**, 347–348 (1991).
35. S. Lunak, J. Vladyka, and K. Dusek, *Polymer*, **19**, 931 (1978).
36. K. Horie, H. Hiura, M. Sawada, I. Mita, and H. Kambe, *J. Appl. Polym. Sci.*, **8**, 1357 (1970).
37. H. E. Adabbo and R. J. J. Williams, *J. Appl. Polym. Sci.*, **27**, 1327 (1982).
38. L. C. Chan, H. N. Nae, and J. K. Gillham, *J. Appl. Polym. Sci.*, **29**, 3307 (1984).
39. J. K. Gillham, *Polym. Engr. & Sci.*, **26**(20), 1429 (1986).
40. G. Wisanrakkit and J. K. Gillham, *J. Appl. Polym. Sci.*, **42**, 2453 (1991).
41. N. Kinjo, M. Ogata, K. Nishi, and A. Kaneda, in Advances in Polymer Science, 88, K. Dusek, Ed., Springer-Verlag, Heidelberg, 1989.
42. X. Wang and J. K. Gillham, *J. Coat. Tech.*, **64**, 37 (1992).

Received March 11, 1992
Accepted March 20, 1992